

Two-dimensional magnetic ordering in a multilayer structure

M K MUKHOPADHYAY and M K SANYAL

Surface Physics Division, Saha Institute of Nuclear Physics, 1/AF Bidhan Nagar,
Kolkata 700 064, India

E-mail: milank.sanyal@gmail.com

Abstract. The effect of confinement from one, two or from all three directions on magnetic ordering has remained an active field of research for almost 100 years. The role of dipolar interactions and anisotropy are important to obtain, the otherwise forbidden, ferromagnetic ordering at finite temperature for ions arranged in two-dimensional (2D) arrays (monolayers). We have demonstrated that conventional low-temperature magnetometry and polarized neutron scattering measurements can be performed to study short-range ferromagnetic ordering of in-plane spins in 2D systems using a multilayer stack of non-interacting monolayers of gadolinium ions formed by Langmuir–Blodgett (LB) technique. The spontaneous magnetization could not be detected in the heterogeneous magnetic phase observed here and the saturation value of the net magnetization was found to depend on the sample temperature and applied magnetic field. The net magnetization rises exponentially with lowering temperature and then reaches saturation following a $T \ln(\beta T)$ dependence. The $T \ln(\beta T)$ dependence of magnetization has been predicted from spin-wave theory of 2D in-plane spin system with ferromagnetic interaction. The experimental findings reported here could be explained by extending this theory to a temperature domain of $\beta T < 1$.

Keywords. Two-dimensional magnetism; neutron scattering; Langmuir–Blodgett films; sub-Kelvin magnetometry.

PACS Nos 75.70.Ak; 75.60.Ej; 75.50.Xx

1. Introduction

Studies of the effect of confinement in nano-magnetic materials are important to refine our basic knowledge in low-dimensional physics. Following the first argument by Bloch in 1930, Mermin–Wagner [1] and later Berezinskii [2,3] predicted in a series of papers that the spontaneous long-range ferromagnetic or antiferromagnetic ordering cannot exist at finite temperature in one- or two-dimensional (1D or 2D) systems, when the spin–spin interaction is mediated only through isotropic exchange coupling. This prediction along with the subsequent theoretical development [4–10] opened a new challenge to the experimentalists. Recent advances in material growth techniques such as the molecular beam epitaxy (MBE) and magnetization measurement techniques like magneto-optical Kerr effect (MOKE) have enabled us

to measure small magnetic signals as a function of magnetic field (H) and temperature (T) even from one atomic monolayer of ferromagnetic materials deposited on a non-magnetic substrate [6,11]. Excellent experiments have been performed on thin films of various ferromagnetic materials ranging from iron to gadolinium and a wide range of ordering effects has been observed [6,8,12]. These measurements have also demonstrated the existence of a spontaneous magnetization and have revealed hysteresis curves in two- [11,13–16] or one-dimensional [17] systems, where magnetic ions are arranged in a grid or a line within a monolayer. However, one can argue that the apparent contradiction between theory and experiment basically arises due to the fact that the ferromagnetic monolayers are not an ideal two-dimensional (2D) system primarily because monolayers are intrinsically anisotropic. Dipole–dipole long-range interaction exists among ions of a monolayer and an additional complication in magnetic ordering arises through substrate–monolayer interactions [11,13,17]. A theoretical formalism [6,8,12] and computer simulations [6,18,19] have been developed to include anisotropy and dipole interactions to explain the apparent contradiction between theory and experiment in ferromagnetic ordering of low-dimensional systems. However, at least two important theoretical predictions of 2D systems remain unverified. These are: the absence of long-range ferromagnetism with the spins aligned in the plane of a monolayer and the $T \ln(\beta T)$ dependence of the magnetization to reach saturation value instead of the linear dependence observed in experiments [5,6]. The primary problem in these experiments arises from the fact that the amount of ferromagnetic material in monolayers is so small that one cannot carry out conventional quantitative magnetization measurements at sub-Kelvin temperatures and by the traditional techniques of polarized neutron scattering [20,21].

Pomerantz *et al* [22] demonstrated that one could form literally isolated two-dimensional (2D) magnets using Langmuir–Blodgett (LB) films. Using LB film growth technique, one can form 2D hexagonal lattice of metallic ions and multilayer stack of these 2D lattices can be kept separated by organic chains [23,24] (figure 1). Several magnetic ions like manganese [25], iron [26], cobalt [27] have been used to form LB films and both the conventional magnetic measurements and the neutron scattering experiments [28] have been done on the LB films. Nicklow *et al* [28] studied neutron diffraction of MnSt_2 multilayer LB films and fitted the curve with a model of ferromagnetically aligned in-plane monolayers having moments lying in the plane and antiferromagnetically aligned alternate planes of Mn monolayers. Due to the lower instrumental resolution and absence of high q_z data, definite conclusion could not be drawn regarding the magnetic ordering in these 2D Mn lattices. Pomerantz *et al* [26] also prepared ferric stearate salts in powder form and found that the magnetization scaled as H/T in the temperature region $295 \text{ K} < T < 60 \text{ K}$ indicating a superparamagnetic interaction between the ferric ions. But below 50 K there were deviations from this scaling behavior and also splitting of the Mössbauer spectrum, indicating a transition to a state of time-independent magnetic order. The susceptibility measurements [25] of MnSt LB films indicated an antiferromagnetic ordering with Néel temperature $T_N = 10 \text{ K}$. Faldum *et al* [29] prepared Fe/Ni multilayer LB films and studied the magnetization using Mössbauer spectroscopy. Giesse *et al* [30] studied the iron arachidate LB films and observed antiferromagnetic ordering in the LB structure. Recently, Hatta

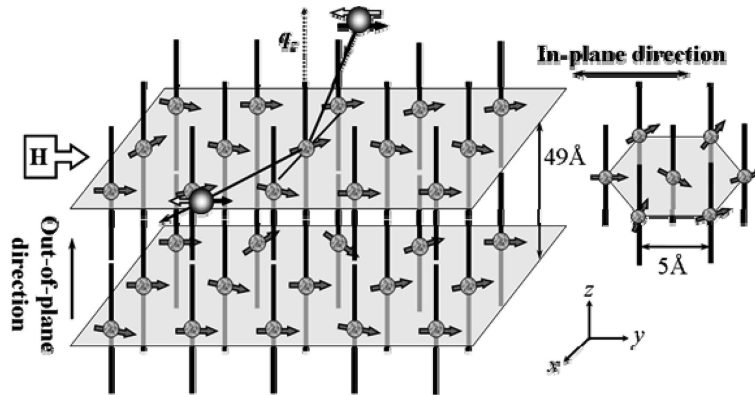


Figure 1. Schematic diagram of the out-of-plane and in-plane structure of the gadolinium stearate Langmuir-Blodgett film is shown with the scattering geometry employed for the polarized neutron reflectivity measurements. xz plane is the scattering plane and the magnetic field is applied along the $+y$ direction. $q_z = (4\pi/\lambda) \sin \alpha$, where λ and α are the wavelength of the radiation and angle of incidence respectively.

et al [27] investigated the CoSt LB films and found spin-glass like behavior in Co lattice. Another recent experiment in gadolinium-based LB films showed the signature of magnetic ordering at unusually high temperature [31]. But due to doubtful stoichiometry and absence of systematic low-temperature magnetic measurements, the nature of ordering could not be established.

The magnetic properties of solids based on gadolinium, a lanthanide metal, are primarily determined by the localized 4f moments. One can observe long-range magnetic ordering here provided the exchange coupling is mediated by the hybridized 6s and 5d conduction electrons [17,32]. On the other hand, one expects to observe paramagnetism [33] in gadolinium compounds due to the absence of conduction electrons. In a recent systematic angle-resolved photoemission measurement of oxygen-induced magnetic surface states of lanthanide metals, it was shown [34] that gadolinium forms GdO instead of non-metallic sesquioxide Gd_2O_3 . The remaining one valence electron of $5d6s^2$ hybridized state was found to be responsible for mediating exchange coupling to form magnetic ordering. In metal-organic structures formed by Langmuir-Blodgett (LB) techniques [23,24,35], metal ions are separated by approximately 5 Å within a monolayer to form a distorted hexagonal 2D lattice and the monolayers are separated from each other by 49 Å by organic chains (refer figure 1).

2. Sample preparation and X-ray characterization

Gadolinium stearate LB films, having 9 to 101 monolayers (ML), were deposited on 1 mm thick Si(001) substrates using an alternating trough (KSV5000) from a monolayer of stearic acid on Milli-Q (Millipore) water subphase containing 5×10^{-4} M Gd^{3+} ions, obtained from dissolved gadolinium acetate. The surface pressure

was maintained at 30 mN m^{-1} during deposition and the dipping speed was 5 mm min^{-1} . The silicon substrates were cleaned and hydrophilized according to RCA cleaning procedure. Grazing incidence X-ray reflectivity measurements were performed using a rotating anode X-ray set-up (ENRAF, Nonius), to characterize the structure of the deposited LB films [24]. In figure 1 we have shown the model of out-of-plane and in-plane structure of GdSt LB films on hydrophilic substrate.

The room temperature X-ray measurements for a 9 monolayer (ML) GdSt LB film are shown in figure 2 with the fitted curves calculated using a simple model (refer figure 1). In these data the presence of both Bragg peaks and Kiessig fringes corresponding to out-of-plane metal-metal distance and total film thickness [36], respectively, are evident. For films with large number of layers, Bragg peaks become strong and Kiessig fringes could not be resolved properly (refer 51 ML data in figure 2). The measured 9 ML data match quite well with the theoretical reflectivity calculated from the electron density profile (refer lower inset of figure 2) of the model shown in figure 1. The organic portion (tail) of the film has electron density of $0.32 \text{ el } \text{\AA}^{-3}$ and dip corresponding to the tail-tail interface going to the value of $0.17 \text{ el } \text{\AA}^{-3}$, as observed earlier [36]. We have also shown the calculated reflectivity data in figure 2 assuming that three tails are attached to a single gadolinium ion. The essential difference between two density profiles is the change of electron density in the metal plane from $0.64 \text{ el } \text{\AA}^{-3}$ to $0.48 \text{ el } \text{\AA}^{-3}$. From these curves, we conclude that out of the three valence electrons in gadolinium only two electrons are participating in bonding with stearic acid. Diffuse scattering data of these films (refer to upper inset of figure 2) show clearly that the 2D metal planes are conformal in nature and have logarithmic in-plane correlation, as observed earlier [37]. The interfacial roughness comes out to be around 2 \AA .

3. Magnetization measurements

The DC magnetization measurements at temperature down to 2 K were carried out using a 12 T commercial (Oxford Instruments) vibrating sample magnetometer (VSM) as a function of magnetic field (H). Magnetization isotherm measurements (M vs. H at a fixed temperature) over all four quadrants including the virgin curve were carried out as a function of magnetic field up to $\pm 70 \text{ kOe}$, applied parallel (in-plane) as well as perpendicular (out-of-plane) to the film plane at several temperatures down to 2 K . All isotherm magnetization measurements were carried out by cooling the sample from 300 K to the desired temperature of measurement under zero magnetic field. Field-cooled (FC) M vs. T magnetization measurements were also carried out over 2 to 100 K under 500 Oe in the cooling cycle.

The DC magnetization measurements at sub-Kelvin temperature were carried out in a Faraday force magnetometer as a function of magnetic field and temperature [38,39]. A cylindrical magnet has been used to apply the field up to 10 T and the sample was mounted on ultra-pure Ag plate vertically to get the in-plane magnetization information of the sample. The sample temperature was varied from 1.5 K down to 30 mK . The field-cooled (FC) and zero-field-cooled (ZFC) data have been taken by cooling the sample from 1.5 K to the base temperature 30 mK in the presence (in the case of FC) or absence (in the case of ZFC) of applied field and all

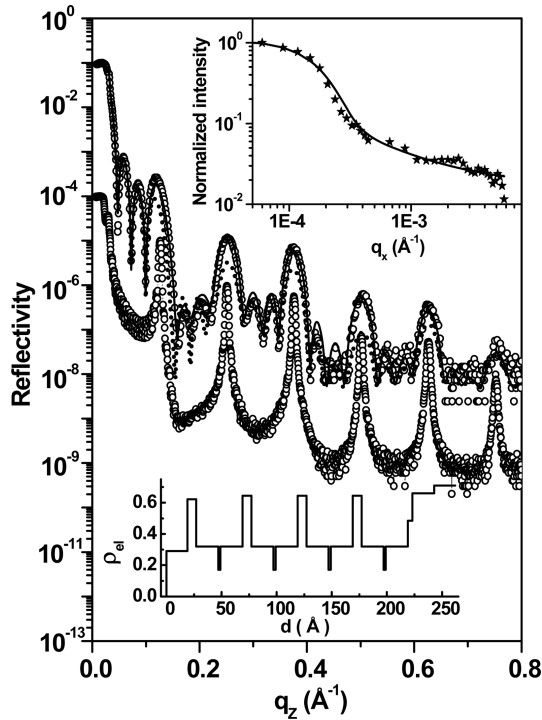


Figure 2. The experimental X-ray reflectivity data points (circles) for 9 ML GdSt LB film and the curve calculated (solid line) with an electron density profile (shown in the lower inset) of the model shown in figure 1. The dashed line is the calculated reflectivity curve corresponding to a model where three stearic acid tails are attached to a gadolinium ion. Reflectivity data of a 51 ML sample (line+star) is also shown for comparison. These data have been shifted down for clarity. Upper inset is the diffuse scattering data of a 51 ML sample fitted with a hypergeometric line profile (refer to text).

the data were collected during heating of the sample. Experiments during cooling of the sample also have been done but no temperature hysteresis was observed.

Neutron reflectivity measurements were carried out in the CRISP reflectometer at the Rutherford Appleton Laboratory (RAL), UK using a cold, polychromatic neutron beam [40,41] and in the ADAM beamline [42,43] of the Institut Laue-Langevin (ILL), Grenoble, France, using a monochromatic cold neutron beam. In CRISP reflectometer the sample was placed in a helium cryostat and an incident wavelength range of 1.2 to 6.5 Å of the incident neutron flux has been used. Three different glancing angles 0.25°, 0.65° and 1.5° were used to collect the specular reflectivity data at a fixed temperature 4.2 K, where the field was allowed to vary from 0 to 15 kOe. In ADAM beamline, the specular reflectivity data were collected using monochromatic neutron beam at different sample temperatures from room temperature to 1.75 K and also for different field values from 0 to 20 kOe.

The polarization of the incident neutrons was either parallel (+) or antiparallel (−) to the applied (along + y axis) field H in all these measurements. In ADAM beamline we carried out spin-flip (SF) analysis of reflected neutron as a function of H by measuring reflectivity profiles R^{+-} ($\sim R^{-+}$) as a function of $q_z = (4\pi/\lambda) \sin \alpha$, α being the angle of reflection as shown in figure 1 [20,21,44,45]. The SF intensity profile is of purely magnetic origin and provides information about the component of the average moment (μ_x) in the in-plane direction (+ x in figure 1) perpendicular to the applied field. In this geometry the effective scattering lengths b_{eff} become equal to $A\mu_x$ and $(b_{\text{coh}} \pm A\mu_y)$ with $A = 0.2695 \times 10^{-4} \text{ \AA}/\mu_{\text{B}}$ for SF ($R^{+-} \sim R^{-+}$) and non-spin-flip (NSF) (R^{++} or R^{--}) reflectivity. We have used well-known convention of polarized neutron reflectivity (R) where first and second superscripts indicate polarization of incident and scattered neutrons, respectively.

4. In-plane and out-of-plane magnetization

In this section we shall discuss the results of the VSM study of these films carried out down to 2 K temperature [35]. The M vs. T curves measured at 500 Oe field in two in-plane (xy) directions, obtained by rotating the film by 90° , and in the out-of-plane (z) direction show a magnetic ordering below 30 K (refer figure 3a). Silicon background was subtracted from all the data consistently before performing data analysis. By studying the other samples, it is found that the magnetization value scales with the number of monolayers deposited where the nature of magnetic ordering is found to be independent of the number of monolayers. Figure 3b shows out-of-plane magnetization data measured at temperatures 5, 10 and 20 K. All the magnetization data plotted against H/T collapse to a single curve as expected for paramagnetism or superparamagnetism. The data were fitted with the expression $M = M_s B_s(g\mu_{\text{B}}SH/k_{\text{B}}T)$, where $M_s (= Ng\mu_{\text{B}}S/V)$ is the saturation magnetization and B_s is the Brillouin function. The value of spin S is found to be 2.75 instead of the expected 3.5 of the 4f moment for gadolinium. The value of M_s was found to be $1.29 \times 10^{-5} \text{ emu/mm}^2$. This value corresponds well with the number of gadolinium per unit area ($\sim 2.53 \times 10^{14} \text{ mm}^{-2}$) as obtained from fitting of the specular reflectivity data (refer figure 2).

In figure 3c magnetization data taken at various temperatures by applying field in a fixed in-plane direction are shown. It is interesting to note that the slope of the curves as well as the respective saturation magnetization (M_s) values decrease as the temperature is increased. As a result, the in-plane magnetization curves do not collapse to a single curve like the out-of-plane data ruling out the existence of normal paramagnetism or superparamagnetism in these 2D planes. However, like in out-of-plane data, no hysteresis (i.e. zero remanent magnetization and zero coercive field) was observed here. It should be noted here that field values (H_s) at which saturation of magnetization sets in was found to decrease with decreasing temperature and these values are 10.2, 21.9, 34.6 and 57.2 kOe for sample temperatures of 2, 5, 10 and 20 K, respectively. This type of field-induced ferromagnetism has been observed earlier [11].

The field-induced saturation magnetization was found to exhibit exponential dependence with temperature ($\log M_s = 0.66 - 0.034T$) (refer inset of figure 3b). Here

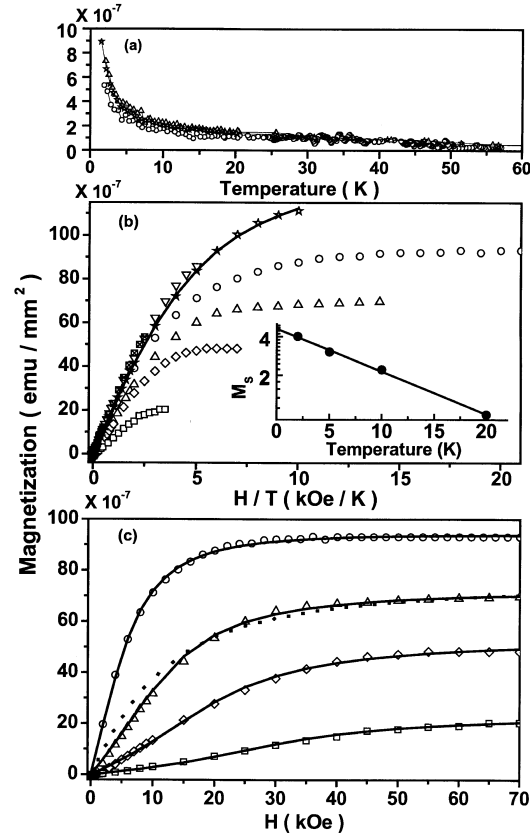


Figure 3. (a) The in-plane magnetization data in two orthogonal directions (line+star) and (line+triangle) respectively and out-of-plane magnetization data (line+circle) measured as a function of temperature (T) with an applied field (H) of 0.5 kOe. (b) Magnetization curves as a function of H/T for the out-of-plane direction measured at 5 K (open star), 10 K (open down-triangle) and 20 K (crossed square) with fit (solid line) using Brillouin function for paramagnetism, and for the in-plane direction measured at 2 K (open circle), 5 K (open up-triangle), 10 K (open diamond) and 20 K (open square). The inset shows log-linear plot of the in-plane saturation magnetization (M_s) expressed in Bohr magneton per gadolinium ion at various temperatures and solid line is the linear fit. (c) In-plane magnetization data as shown in (b) are plotted against field with the corresponding fit (line) using eq. (3). The dotted line is the best-fitted Brillouin function with field independent exchange (refer text).

M_s is expressed in μ_B/Gd and the projected value of M_s at 0 K comes out to be $4.57 \mu_B/\text{Gd}$. This value is less than the value of 5.5 obtained from the fitting of out-of-plane data. We shall discuss this exponential dependence of magnetization while presenting neutron and sub-Kelvin data in the later sections. An explanation of our observations has been given based on a mean-field like model [35]. Absence

of spin-spin interaction when the field is applied in the out-of-plane (z) direction is accommodated in this model by considering *anisotropic exchange*

$$\mathbf{J}\mathbf{S}_i \cdot \mathbf{S}_j = J_x S_i^{(x)} S_j^{(x)} + J_y S_i^{(y)} S_j^{(y)} + J_z S_i^{(z)} S_j^{(z)} \quad (1)$$

with $J_z = 0$. As LB films are essentially powder in the 2D plane having about 100 Å domain size, it is assumed that in the xy -plane, the exchange is isotropic, i.e., $J_{\parallel} = J_x = J_y$.

Brillouin function as used in ferromagnetism [5] can be utilized to write magnetization in the in-plane direction noting that $J_z = 0$ and by neglecting spin fluctuations $(S_i - \langle S_i \rangle)(S_j - \langle S_j \rangle)$,

$$M = M_s B_s \left(\frac{S}{k_B T} \left[g \mu_B H + J_{\parallel} \langle S_j \rangle^{\parallel} \sum_j \cos \theta_{ij} \right] \right), \quad (2)$$

where θ_{ij} is the angle between spins S_i and S_j . The thermal averaged value of the in-plane component $\langle S_j \rangle^{\parallel}$ will increase to the maximum value of S with the field H applied in an in-plane direction and approximated this component as $CH \langle S_j \rangle$. In the next section we shall discuss the polarized neutron scattering results that clearly show that the angle θ_{ij} is essentially in y - z plane. Even with small H , the x component of spin becomes negligible. With increasing applied field the *sum of cosines*, in eq. (2) gets maximized. All these relationships can be used to write a simplified transcendental equation for in-plane magnetization as

$$M = M_s B_s \left(\frac{SH}{k_B T} \mu_B (g + J_{\parallel} C M) \right). \quad (3)$$

The constant C used in this linear approximation will depend on the angle, if any, between H and the xy plane of the LB film. If H is applied normal to the xy plane, C will become zero and from eq. (3) we get back the expression of paramagnetism. The value of C is also expected to depend on temperature. It should be noted here that without invoking this field-dependent exchange term the data could not be analysed. The fitting of the data with a Brillouin function having constant exchange term 1.27×10^6 kOe mm² emu⁻¹ for the 5 K data was obtained and showed by the dotted curve in figure 3c. In figure 3c measured M along with the fitted curves obtained by using eq. (3) for 2, 5, 10 and 20 K data was plotted. In this analysis $S = 3.5$ was used and the only fitting parameter was $J_{\parallel} C$, which increases with increasing temperature. The values come out to be 2.45×10^4 , 8.82×10^4 , 2.15×10^5 and 8.28×10^5 mm² emu⁻¹ at temperatures 2, 5, 10 and 20 K respectively. It is expected that the exchange will not increase from 2 to 20 K and hence with increasing temperature C is increasing making field-induced in-plane spin alignment easier at elevated temperatures.

5. Results from polarized neutron scattering

Typical spin-polarized neutron reflectivity data taken at 2 K by applying a magnetic field of 13 kOe are shown in figure 4a. In the left inset of figure 4a we have

shown reflectivity profiles of parallel (+) and anti-parallel (−) incident neutrons at the first peak position. In the right inset of figure 4a we have shown peak-normalized transverse diffuse neutron scattering intensity profile at the first Bragg peak. Transverse diffuse scattering intensity provides us information regarding the nature of surface roughness through height–height correlation function and neutron diffuse scattering can in principle determine magnetic and structural contributions in roughness. The hyper-geometric lineshape profile confirms that the in-plane correlation is logarithmic in nature and that the interfaces are conformal [46,47]. It should be noted that unlike in X-ray measurements the scattering here originates primarily from the metal heads. The lineshape and the associated parameters were found to be independent of T , H and hence magnetic contribution in roughness is negligible here. This again confirms that the GdSt LB films represent a collection of isolated 2D spin membranes of gadolinium ions. In figure 4b we have shown two sets of NSF and SF transverse data (R^{++} and R^{+-}) of the first Bragg peak collected at $T = 2$ K by applying a field of 2 kOe and 13 kOe. Negligible intensity in SF data (R^{+-} or R^{-+}) clearly indicate that $\langle\mu_x\rangle$ component is not detectable and all the reflectivity profiles (collected without analysing the spin of scattered neutrons) can be analysed [48,49] with $b_{\text{eff}} = b_{\text{coh}} \pm A\mu_y$, where μ_y represents average moment per gadolinium ion along field direction (+ y axis).

Systematic analysis of all the reflectivity profiles provide us values of μ_y as a function of H at 4.2 K and at 1.75 K obtained in the CRISP and ADAM spectrometers respectively. The results are shown in figure 5a with the results obtained from earlier magnetization measurements [35] carried out at 2 K and 5 K. Results of these two independent measurements [48] show that the obtained average saturated moment per gadolinium ion is consistent with earlier data and much less than the expected value of $7 \mu_B$. The μ_y values obtained from neutron reflectivity data and magnetometry data obtained earlier [35] clearly show that saturation moment increases with lowering temperature. In figure 5a we have also presented the M vs. H data collected at the temperatures 100 mK and 500 mK. The saturation value of the net magnetization at 100 mK and 500 mK is found to reach the same value of $12.7 \times 10^{-6} \text{ emu/mm}^2 \approx 5.4 \mu_B/\text{Gd atom}$; much lower than the expected $7.0 \mu_B/\text{Gd atom}$ for a homogeneous phase. However, it may be noted that this value is close to the saturation magnetization value obtained by fitting paramagnetic data obtained in out-of-plane direction [35]. In figure 5a we have also plotted magnetization data collected at 5 K temperature earlier [35] along the growth direction (+ z direction) that exhibits paramagnetism. Magnetization value of in-plane data is always lower than that of growth direction (+ z direction) for the same temperature at each applied field, indicating that it is hard to keep the spins in xy plane. But exchange interaction resulting in saturation of moment becomes evident only when spins are kept in xy plane [35]. The absence of hysteresis and remanence ($M = 0$ at $H = 0$) is apparent in magnetization data although saturation magnetization is observed in all in-plane data.

We performed [49] systematic M vs. T measurements for investigating the nature of magnetic ordering of in-plane spins forming a heterogeneous phase in the gadolinium monolayer. M vs. T was first measured using neutron reflectivity technique at a fixed field $H = 13$ kOe and values of the component of average moment μ_y obtained from the analysis of the reflectivity profiles at different temperatures

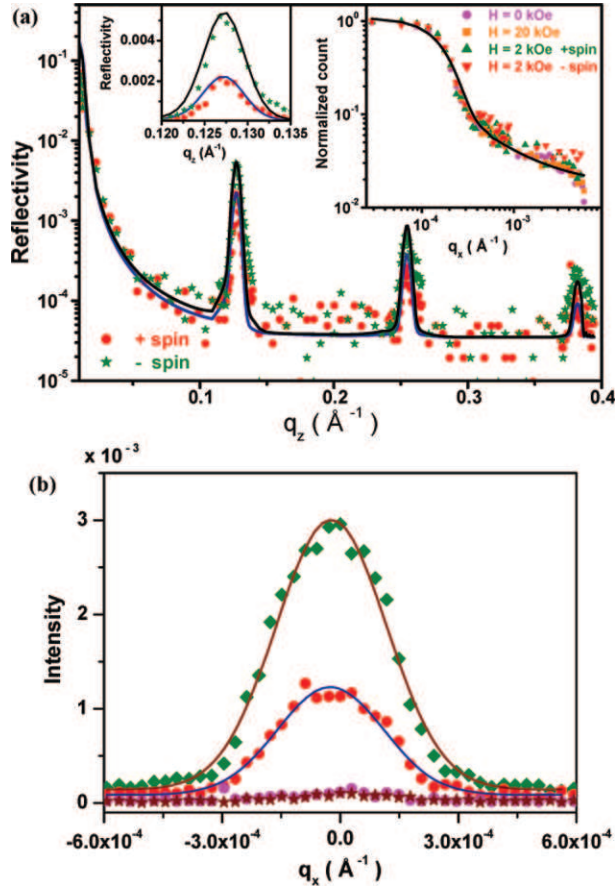


Figure 4. (a) Neutron reflectivity data (symbols) at $H = 13$ kOe and at $T = 2$ K for the neutron spin along (+) and opposite (-) to the magnetic field direction with the corresponding fit (line). In the left inset the first Bragg peak is shown in (+) and (-) channels in an expanded scale. Right inset: Transverse diffuse neutron scattering profiles (symbols) measured at 2 K with unpolarized and polarized neutron beams. The solid line is a fitted hypergeometric curve as described in the text. (b) Transverse diffuse neutron scattering profiles for + (green diamonds) and - (red circles) spin state of the incident neutrons at $T = 2$ K and $H = 13$ kOe. Transverse diffuse neutron scattering profiles in SF channel for the applied fields $H = 2$ kOe (pink circles) and 13 kOe (brown stars) at $T = 2$ K are also shown. The solid line is guide to eye.

are shown in figure 5b along with a fit by an exponential function. The magnetization extracted from the reflectivity data shows that the magnetization and hence the percentage of ordered majority phase increase exponentially with the decrease in temperature. It is known that both the average magnetization $M(T)$ as well as the initial susceptibility $\chi(T)$ are proportional to the physical extent (l^*) of the

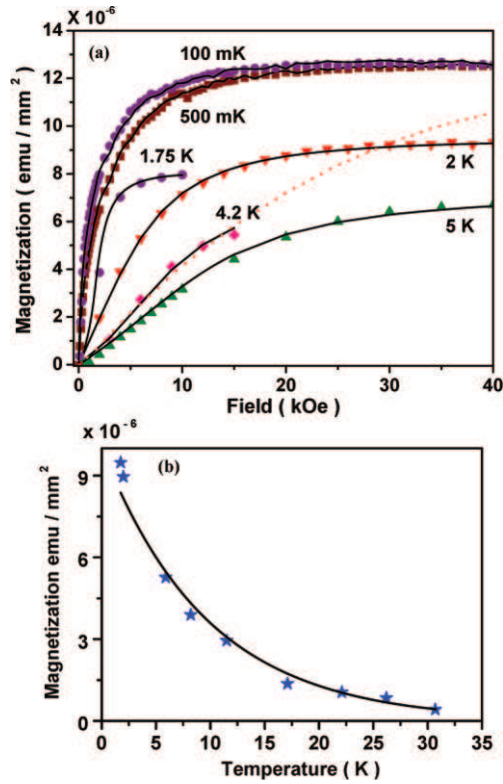


Figure 5. (a) In-plane magnetization curves obtained as a function of the field (H) using neutron reflectivity measured at 4.2 K (diamond) and 1.75 K (star) compared with conventional magnetization data [35] measured at 2 K (down-triangle) and 5 K (up-triangle). Solid lines are the fits with a modified Brillouin function [35]. Magnetization measured at 100 mK and 500 mK are shown for the 1st (symbols) and 2nd (line) cycle of the hysteresis loop. Red dotted line is the magnetization curve when the applied field is in the out-of-plane (z) direction. (b) The magnetization obtained from neutron reflectivity measurements as a function of temperature (symbols) and fit with eq. (4) (line).

ordered phase that minimizes the zero-field energy [6] and can be written as

$$M \propto Hl^* \text{ and } \chi \propto l^* \text{ with } l^* \propto \exp(-\gamma T). \quad (4)$$

It is expected that at low enough temperature, the correlation length l^* reaches saturation either because l^* becomes comparable to the sample size or due to a freezing of the walls of in-plane domains. This explains our observation of exponential dependence of magnetization with temperature, where l^* for the gadolinium lattice remains lower than the sample dimension even for the highest field and lowest temperature used here (figure 5b).

6. Sub-Kelvin magnetization measurement

We have carried out [49] M vs. T measurements using Faraday balance [38] to investigate the nature of ordering below the temperature where correlation length l^* saturates. In figure 6a we have shown the magnetization data taken with different applied fields as a function of temperature. The higher temperature region of the M vs. T curves taken with fields of 0.25, 0.5 and 1.0 kOe exhibited exponential behavior as observed in neutron measurements and were fitted with eq. (4). It is also observed that at a lower field, the magnetization at a fixed temperature is nearly proportional to the applied field (5.03×10^{-7} at 0.25 kOe and 1.29×10^{-6} emu/mm² at 0.5 kOe and at a temperature of 0.9 K) as predicted by eq. (4). The values of γ obtained from fitting were found to increase with the reduction of H and at 0.25 kOe, it is found to be 2.162 K^{-1} . But below a certain temperature (T_w) corresponding to each field ($\sim 450 \text{ mK}$ and 600 mK for the applied fields 0.5 and 1.0 kOe respectively) the growth of l^* stops possibly due to the freezing of the domain walls of the ordered phase. Below this temperature, the measured data show much slower increase in M with lowering temperature than predicted by eq. (8). This transition temperature (T_w) shifts toward higher temperature as the field increases and we do not have appreciable temperature region of the M vs. T curves at $H = 2.5$ and 5.0 kOe (refer to figure 6a) that shows exponential behavior. We have discussed in the next section the fitted curves (wine colored lines), shown in figure 6a. All these data give us different saturation magnetization (M_0) values depending upon the H values used to take the data. We obtained M_0 values as 0.9×10^{-6} , 1.6×10^{-6} , 3.2×10^{-6} , 4.5×10^{-6} , 7.9×10^{-6} , 9.5×10^{-6} emu/mm² with 0.15, 0.25, 0.5, 1.0, 2.5, 5.0 kOe magnetic fields respectively. These saturation values of net magnetization indicate that the percentage of the ordered phase is increasing from 7.1 to 74.8% as we approach the maximum saturation value of net magnetization 12.7×10^{-6} emu/mm² ($\approx 5.4 \mu_B/\text{Gd atom}$) as shown in figure 6a. As any in-plane direction is hard axis for all these films, one needs to apply field to keep spins in xy plane. We obtained lower M_0 values for lower field (figure 6a) and higher temperature (figure 5a) as spins get oriented along out-of-plane direction, which is the easy axis. In figure 6b we have shown zero-field-cooled (ZFC) and field-cooled (FC) magnetization data taken with 0.15 kOe and 0.5 kOe field. We observe a temperature of 125 mK below which there is branching in the ZFC and FC data. These data are consistent with the fact that one needs a field to keep the spins in xy plane and this branching is not observed when 0.5 kOe or higher field was used.

7. The proposed model

All our experimental observations point to the fact that any in-plane direction is not the easy axis of magnetization and there is a strong crystalline anisotropy present in the system to keep spins along the out-of-plane ($\pm z$) direction. Spin-flip data obtained in polarized neutron scattering clearly showed that even with small field spins become confined in yz plane. As a result, the magnetization data could not be analysed using Kostreerliz-Thouless (KT) theory for xy model [50,51]. Hence applied field, exchange, anisotropy and dipolar interaction play crucial roles

in establishing the short-range ferromagnetic ordering of in-plane spins, observed here.

We can use a 2D array of magnetic ions with lattice parameter a of spins S to explain our observation with a Hamiltonian,

$$H = H_{\text{ex}} + H_{\text{d}} + H_{\text{k}}. \quad (5)$$

The strength of the three terms arise from exchange, dipolar and magneto-crystalline anisotropic interactions respectively, and have been approximated by expressing [5,6] these terms in equivalent magnetic field units as

$$2\mu_{\text{B}}H_{\text{ex}} = JS, \quad 2\mu_{\text{B}}H_{\text{d}} = 4\pi\alpha g'S, \quad 2\mu_{\text{B}}H_{\text{k}} = 6KS. \quad (6)$$

In the above expression, α (~ 1) depends on the lattice type and g' is equal to $(2\mu_{\text{B}})^2/a^3$ [6], K is the anisotropy constant. The reduction in magnetization due to thermally activated spin waves was calculated with this Hamiltonian and the axis of easy magnetization is determined by the sign of the effective anisotropy field ($H_{\text{k}}^{\text{eff}} = H_{\text{k}} - H_{\text{d}}$), which is defined [8] as

$$H_{\text{k}}^{\text{eff}} = \frac{1}{2\mu_{\text{B}}}(6K_{\text{eff}}S) \quad \text{with} \quad K_{\text{eff}} = K - \frac{2\pi\alpha g'}{3}. \quad (7)$$

For $H_{\text{k}}^{\text{eff}} > 0$ and $H_{\text{k}}^{\text{eff}} < 0$, the magnetization lies perpendicular to the plane and in the in-plane respectively. The long-range character of the dipole interactions was found [7] to be responsible for creating a pseudogap $\Delta_{xy} = (\pi Sg'/2)\sqrt{(6|K_{\text{eff}}|/J)}$ in the spin-wave spectrum that may give rise to ferromagnetic order in 2D in-plane spins. The stability criterion for the homogeneously magnetized state for obtaining the in-plane spins is $|K_{\text{eff}}| > K_{\text{c}} = \pi^2 g'^2/(6J)$. The temperature dependence of the magnetization $M(T)$ above a transition temperature $T_{\text{c}} (= 6S|K_{\text{eff}}|/K_{\text{B}})$ takes the form [49]

$$M(T) = M_0[1 - AT \ln(\beta T)] \quad (8)$$

for the ordering of in-plane spins (with $\beta = K_{\text{B}}/\Delta_{xy} = 2\sqrt{6|K_{\text{eff}}|J}/(\pi g'T_{\text{c}})$). Here $A = K_{\text{B}}/(4\pi JS^2)$ and M_0 is the saturation value of the net magnetization that depends on the field applied to carry out measurements [52]. Below T_{c} spin-wave theory predicts [8] an enhancement of $M(T)$ as $M_0[1 - CT^v]$ for in-plane ordering where C depends on Δ_{xy} and v is expected to be $3/2$ [6-8]. For $0 < |K_{\text{eff}}| < \pi^2 g'^2/(6J)$ in-plane spins cannot stabilize in a homogeneous phase as the magneto-crystalline anisotropy becomes large enough to pull some of the spins in the out-of-plane direction and create a ripple-like instability [6,8]. This results in the formation of ferromagnetic domains, as observed here. The net magnetization $M(T)$ is then a sum of magnetization of each of these ordered domains. $M(T)$ should follow the spin-wave prediction (eq. (8)) to reach saturation, if we assume that sizes of the domains are not increasing during this ripening process.

This assumption is valid as the domain walls freeze below a certain temperature for each field (~ 0.45 and 0.6 K for the applied fields 0.5 and 1.0 kOe respectively). Hence the net magnetization $M(T)$ curves in this lower temperature range could be analysed by eq. (8). We extracted the value of exchange J as 8.76×10^{-19} erg (or

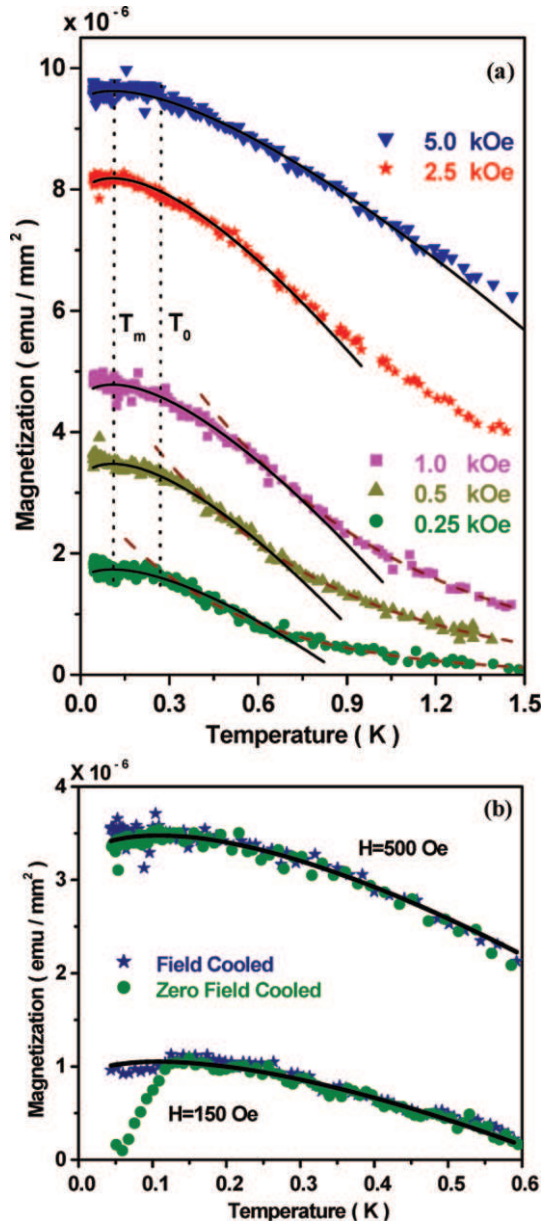


Figure 6. (a) Sub-Kelvin magnetization results with various applied fields (symbols) fitted with eq. (8) (black line) and with eq. (4) (wine colored dashed lines). Dotted lines indicate the temperatures T_m and T_0 (refer to text). (b) ZFC (green circles) and FC (blue stars) along with the fit (line) for FC measurements.

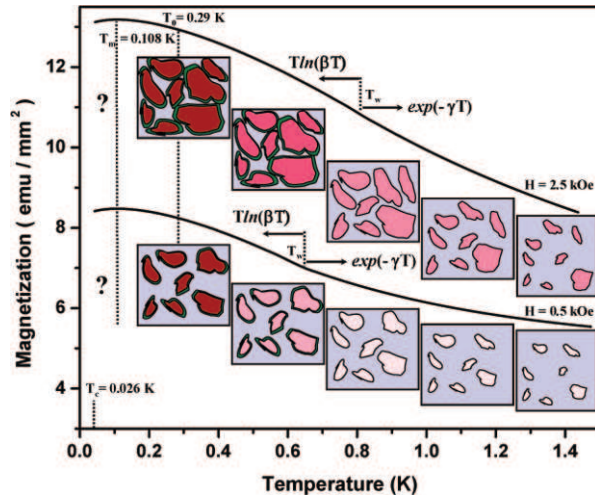


Figure 7. The schematic representation of the results indicating three temperature zones: $T < T_c$ (marked as data could not be taken there), $T_c < T < T_w$ and $T > T_w$. Exponential dependence of magnetization was observed in $T > T_w$ zone due to growth of ordered domains (indicated by pink colour). In $T_c < T < T_w$ short-range ferromagnetic ordering takes place within each domain – this ripening process is indicated by darker shading. We have used two data sets of figure 6a to explain our observation and characteristic temperatures T_c , T_m , T_0 and T_w are also indicated (refer text for details).

$H_{\text{ex}} = 0.165$ kOe) from the fitted value of $A (= 1.02 \text{ K}^{-1})$ for the 0.25 kOe data. We obtained β as 3.4 for all the data and hence $|K_{\text{eff}}|$ was calculated to be 1.7×10^{-19} erg (or $H_{\text{k}}^{\text{eff}} = 0.19$ kOe) for 0.25 kOe data giving $T_c = 26$ mK. In this calculation g was 6.88×10^{-18} erg, assuming that one gadolinium atom occupies $2.5 \text{ \AA} \times 20 \text{ \AA}^2$, as obtained from neutron and X-ray analysis (refer figure 1). These values confirmed that $0 < |K_{\text{eff}}| < K_c (= 8.89 \times 10^{-17}$ erg) and the ferromagnetic ordered phase here is not homogeneous. It is known that eq. (8) describes the temperature dependence of the magnetization for ferromagnetic ordering of both in-plane and out-of-plane spins, but the argument of the logarithmic function can become less than 1 only for in-plane ordering. Unusually low values of H_{ex} and $H_{\text{k}}^{\text{eff}}$ with a rather large value of $H_{\text{d}} (= 16.3$ kOe) make $\beta T < 1$ even for $T > T_c$. It is interesting to note that all the magnetization data shown in figure 6a attains respective saturation values M_0 at temperature $T_0 = 1/\beta$ (≈ 0.29 K) and a maximum magnetization at temperature $T_m = 1/(e\beta)$ (≈ 0.108 K). The experimental uncertainties below 100 mK prohibit us from commenting on the nature of magnetization below this T_m but eq. (8) still can be used to fit the data quite well with same A and β even for the temperature region $\beta T < 1$.

8. Conclusion

We have demonstrated that polarized neutron scattering and conventional magnetization measurements can be used to study 2D ferromagnetic ordering of

in-plane spins using a stack of magnetically uncorrelated spin membranes formed with gadolinium stearate LB film. The in-plane ordering observed here shows that even at 100 mK a spontaneous magnetization could not be detected. We have summarized the observed results and the proposed model in figure 7. The magnetic ordering observed here can be grouped in three temperature zones as $T < T_c$; $T_c < T < T_w$ and $T > T_w$. We could not take data so far in the temperature range below the critical temperature $T_c \approx 26$ mK. In the temperature zone above the temperature T_w , where domain walls freeze, the magnetization is found to increase exponentially with the lowering in temperature. The exponential increase of magnetization indicates the formation of heterogeneous phase in the in-plane Gd lattice where the physical extent of the ferromagnetic domains increases exponentially with lowering temperature. In the temperature zone of $T_c < T < T_w$ the sizes of the domains stop growing due to freezing of the domain walls and the ordering within each of these ferromagnetic domains ultimately saturate following $T \ln(\beta T)$ which is a characteristic of thermally activated spin waves and are found to be valid for even $\beta T \leq 1$. We believe that the results will initiate further studies in low-dimensional magnetic ordering using soft magnetic materials [53].

References

- [1] N D Mermin and H Wagner, *Phys. Rev. Lett.* **17**, 1133 (1966); **17**, 1307 (1966)
- [2] V L Berezinskii, *Sov. Phys. JETP* **32**, 493 (1971)
- [3] V L Berezinskii, *Sov. Phys. JETP* **34**, 610 (1972)
- [4] C M Schneider and J Kirschner, *Handbook of surface science* edited by K Horn and M Scheffler (Elsevier, Amsterdam, 2000), p. 511
- [5] P Bruno, *Phys. Rev. Lett.* **87**, 137203 (2001)
- [6] K De'Bell, A B MacIsaac and J P Whitehead, *Rev. Mod. Phys.* **72**, 225 (2000)
- [7] S V Male'ev, *Sov. Phys. JETP* **43**, 1240 (1976)
- [8] P Bruno, *Phys. Rev.* **B43**, 6015 (1991)
- [9] A Aharoni, *Introduction to the theory of ferromagnetism* (Oxford University Press, New York, 2000)
- [10] Zsolt Gulácsi and Miklós Gulácsi, *Adv. Phys.* **47**, 1 (1998)
- [11] H J Elmers, *Int. J. Mod. Phys.* **B9**, 3115 (1995)
- [12] A Kashuba and V L Pokrovsky, *Phys. Rev. Lett.* **70**, 3155 (1993)
- [13] H J Elmers, G Liu and U Gradmann, *Phys. Rev. Lett.* **63**, 566 (1989)
- [14] H M Bozler, Yuan Gu, Jinshan Zhang, K S White and C M Gould, *Phys. Rev. Lett.* **88**, 065302 (2002)
- [15] S Padovani, I Chado, F Scheurer and J P Bucher, *Phys. Rev.* **B59**, 11887 (1999)
- [16] M R Scheinfein, K E Schmidt, K R Heim and G G Hembree, *Phys. Rev. Lett.* **76**, 1541 (1996)
- [17] P Gambardella, A Dallmeyer, K Maiti, M C Malagoli, W Eberhardt, K Kern and C Carbone, *Nature (London)* **416**, 301 (2002)
- [18] I Booth, A B MacIsaac and J P Whitehead and K De'Bell, *Phys. Rev. Lett.* **75**, 950 (1995)
- [19] A B MacIsaac, J P Whitehead, M C Robinson and K De'Bell, *Phys. Rev.* **B51**, 16033 (1995)
- [20] C G Shull and J S Smart, *Phys. Rev.* **76**, 1256 (1949)

- [21] G P Felcher, *Phys. Rev.* **B24**, R1595 (1981)
- [22] M Pomerantz, F H Dacol and A Segmüller, *Phys. Rev. Lett.* **40**, 246 (1978)
- [23] M K Sanyal, M K Mukhopadhyay, M Mukherjee, A Datta, J K Basu and J Penfold, *Phys. Rev.* **B65**, 033409 (2002)
- [24] J K Basu and M K Sanyal, *Phys. Rep.* **363**, 1 (2002)
- [25] A Aviram and M Pomerantz, *Solid State Commun.* **41**, 297 (1982)
M Pomerantz, *Surf. Sci.* **142**, 556 (1984)
- [26] M Pomerantz, A Aviram, A R Taranko and N D Heiman, *J. Appl. Phys.* **53**, 7960 (1982)
- [27] E Hatta, T Maekawa, K Mukasa and Y Shimoyama, *Phys. Rev.* **B60**, 14561 (1999)
- [28] R M Nicklow, M Pomerantz and A Segmüller, *Phys. Rev.* **B23**, 1081 (1981)
- [29] T Faldum, W Meisel and P Gütlich, *Hyperfine Interactions* **92**, 1263 (1994)
T Faldum, W Meisel and P Gütlich, *Appl. Phys.* **A62**, 317 (1996)
- [30] E Giesse, G Ritter, D Brandl, H Voit and N Rozlosnik, *Hyperfine Interactions* **95**, 175 (1995)
- [31] A M Tishin, Yu A Koksharov, J Bohr and G B Khomutov, *Phys. Rev.* **B55**, 11064 (1997)
A M Tishin, O V Snigirev, G B Khomutov, S A Gudoshnikov and J Bohr, *J. Magn. Magn. Mater.* **234**, 499 (2001)
- [32] B N Harmon and A J Freeman, *Phys. Rev.* **B10**, 1979 (1974)
- [33] W E Henry, *Phys. Rev.* **88**, 559 (1952)
- [34] C Schüßler-Langeheine, H Ott, A Yu Grigoriev, A Möller, R Meier, Z Hu, C Mazumdar, G Kaindl and E Weschke, *Phys. Rev.* **B65**, 214410 (2002)
- [35] M K Mukhopadhyay, M K Sanyal, M D Mukadam, S M Yusuf and J K Basu, *Phys. Rev.* **B68**, 174427 (2003)
- [36] J Daillant and A Gibaud, *X-ray and neutron reflectivity: Principles and applications* (Springer, Berlin, 1999)
- [37] J K Basu, S Hazra and M K Sanyal, *Phys. Rev. Lett.* **82**, 4675 (1999)
- [38] T Sakakibara, H Mitamura, T Tayama and H Amitsuka, *Jpn. J. Appl. Phys.* **33**, 5067 (1994)
- [39] A Harita, T Tayama, T Onimaru and T Sakakibara, *Physica* **B329–333**, 1582 (2003)
- [40] J Penfold and R K Thomas, *J. Phys.: Condens. Matter* **2**, 1369 (1990)
- [41] J P Goff, P P Deen, R C C Ward, M R Wells, S Langridge, R Dalglish, S Foster and S Gordeev, *J. Magn. Magn. Mater.* **240**, 592 (2002)
- [42] H Zabel, *Physica* **B198**, 156 (1994)
- [43] V Leiner, K Westerholt, A M Blixt, H Zabel and B Hjörvarsson, *Phys. Rev. Lett.* **91**, 037202 (2003)
- [44] H Kepa, Kutner-Pielaszek, J A Twardowski, C F Majkrzak, J Sadowski, T Story and T M Giebultowicz, *Phys. Rev.* **B64**, 121302 (2001)
- [45] A Schreyer, Th Zeidler, Ch Morawe, N Metoki, H Zabel, J F Ankner and C F Majkrzak, *J. Appl. Phys.* **73**, 7616 (1993)
- [46] M K Sanyal, S K Sinha, K G Huang and B M Ocko, *Phys. Rev. Lett.* **66**, 628 (1991)
- [47] The measured roughness and ‘true’ roughness [46] of the interfaces are calculated to be 2.3 Å and 5.4 Å respectively and we get an effective surface tension equal to 10 mN/m
- [48] M K Sanyal, M K Mukhopadhyay, R M Dalglish and S Langridge, *Int. J. Nanosci.* **4**, 831 (2005)
- [49] M K Mukhopadhyay, M K Sanyal, T Sakakibara, V Leiner, R M Dalglish and S Langridge, *Phys. Rev. B* (in press)

- [50] J M Kosterlitz and D J Thouless, *J. Phys.* **C6**, 1181 (1973)
J M Kosterlitz, *J. Phys.* **C7**, 1046 (1974)
- [51] R Gupta, J DeLapp, G G Batrouni, G C Fox, C F Baillie and J Apostolakis, *Phys. Rev. Lett.* **61**, 1996 (1988)
- [52] P Bruno, *Mater. Res. Soc. Symp. Proc.* **231**, 299 (1992)
- [53] R C O'Handley, *Modern magnetic materials, principles and applications* (John Wiley, New York, 2000)